文章编号:1672-6553-2023-21(11)-019-008

DOI:10.6052/1672-6553-2023-005

湿热环境下铺设镍钛合金钢丝绳功能梯度梁的振动控制*

张博文　臧健†

(沈阳航空航天大学 航空宇航学院,沈阳　110136)

摘要　本文提出了一种新型阻尼装置镍钛合金钢丝绳,它是一种具有线性阻尼、非线性阻尼的减振器.本研究将镍钛合金钢丝绳减振装置与功能梯度材料梁模型相耦合.采用龙格－库塔法和谐波平衡法分别从数值和解析两方面研究系统的共振响应.验证镍钛合金钢丝绳为功能梯度梁提供的减振效果.改变外部环境的温度和湿度,会影响梁模型的刚度,从而影响共振峰峰值,但不会影响镍钛合金钢丝绳的减振效果.仿真结果证实,镍钛合金钢丝绳是一种很有前景的非线性阻尼器,可作为抑制连续体结构振动的新方法.

关键词　功能梯度梁,　镍钛合金钢丝绳,　振动抑制,　湿热环境

中图分类号:O322　　**文献标志码**:A

Vibration Control of Functionally Graded Beam Coupled with NiTiNOL-Steel Wire Ropes under Hygrothermal Environment*

Zhang bowen　Zang jian†

(College of Aerospace Engineering, Shenyang Aerospace University, Shenyang　110136, China)

Abstract　In this paper, a new type of damping device NiTiNOL-steel wire ropes (NiTi-ST) are proposed. It is a vibration absorber with linear hysteresis damping and nonlinear damping. In this study, the NiTi-ST damping device is coupled with a functionally graded material (FGM) beam model. The Runge-Kutta method and the harmonic balance method are used to study the resonance response of the system from both numerical and analytical aspects. It is verified that NiTi-ST provides an effective vibration reduction effect for FGM beam. Changing the external environment temperature and humidity will affect the stiffness of the beam model, thus affecting the resonance peak value, but will not affect the damping effect of NiTi-ST. The simulation results confirm that NiTi-ST is a promising nonlinear damper and can be used as a new method for vibration suppression of continuous structures.

Key words　functionally graded beam,　NiTiNOL-steel wire ropes,　vibration suppression,　hygrothermal environment

引言

功能梯度材料(functionally graded material, FGM)是一种力学性质随位置变化实现梯度函数变化的新型材料[1].它克服了复合材料层间界面处性能快速转变,导致组分在分层过程中失效的缺点[2].因此,FGM 已广泛应用于工作环境复杂的航空航天领域[3].由于复杂的工作环境,产生大的振

2022-11-23 收到第 1 稿,2023-01-08 收到修改稿.

* 国家自然科学基金资助项目(12272240), National Natural Science Foundation of China (12272240).

† 通信作者 E-mail:zangjian106@163.com

动是不可避免的.这种振动会损坏结构,降低结构的精度和寿命,并造成噪音污染[4].梁板结构作为工程中最常见的承重构件之一,长期以来一直是减振方面的研究热点[5-7].因此,FGM 梁的振动控制是一个亟待关注和解决的问题[8].

常见的振动控制方法主要分为主动隔振法[9,10]、被动振动控制法[11,12]和半主动振动控制法[13].传统的被动控制,如非线性能量阱(nonlinear energy sink, NES)结构[14-16]、准零刚度系统[17,18]、X 型结构[19]等.此类方法的振动控制效果明显,系统的固有频率几乎保持不变.但是它们的主要缺点是不仅需要一定的安装空间和一定的运动行程,而且还增加了结构的额外质量.

形状记忆合金(shape memory alloys, SMA)是一种金属合金,是新型阻尼器的理想材料,具有多种优异的性能,例如通过响应迟滞产生能量耗散,耐腐蚀,高强度和抗疲劳性[20].Carboni 等人提出了一种镍钛合金钢丝绳(NiTiNOL-steel wire ropes,NiTi-ST)是一种在弯曲或拉伸－弯曲耦合条件下具有恢复力和阻尼力的新型减振器[21].使用改进的 Bouc-Wen 模型从理论和实验研究了 NiTi-ST 的非线性力学行为[22,23].Brewick 等人探索了 NiTi-ST 的非线性行为,并使用数据驱动的方法为 NiTi-ST 开发了广义力学模型[24].同时降低了多项式模型的阶数,并取得了与传统方法相同的结果[25].

本文其余的结构安排如下:第 1 节建立 FGM 梁与 NiTi-ST 耦合系统的动力学模型,第 2 节研究梁的自由振动,第 3 节使用伽辽金法(Galerkin truncation method,GTM)将系统控制方程离散化.采用龙格－库塔法(Runge-Kutta method,RKM)和谐波平衡法(harmonic balance method,HBM)在数值和解析两个方面近似求解模型的常微分控制方程.第 4 节比较了在不同温度和不同湿度下 NiTi-ST 对第一阶共振峰的振动抑制.第 5 节总结全文.

1 动力学模型

图 1 显示了弹性欧拉－伯努利梁的结构模型.该梁模型由 FGM 组成,其长、宽和高分别为 L , B 和 H , 梁上铺设有一根 NiTi-ST。FGM 梁两端均为固定端约束.FGM 梁的材料属性 P (如弹性模量 E 、密度 ρ 、热膨胀系数 α 、湿膨胀系数 β 等)基于每个组件的体积沿材料厚度呈指数分布,可以写成

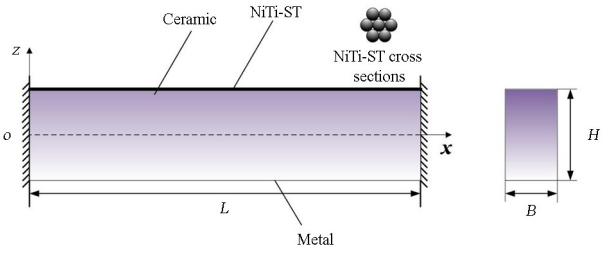

图 1 功能梯度梁与镍钛合金钢丝绳的耦合系统
Fig.1 FGM beam coupled with NiTi-ST

$$P(z)=(P_2-P_1)\left(\frac{2z+H}{2H}\right)^n+P_1 \tag{1}$$

其中 n 是材料的梯度指数, P_1 和 P_2 分别代表上表面陶瓷和下表面金属的材料特性.基于物理中面的概念,模型的物理中面为

$$z=z_0=\frac{\int_{-H/2}^{H/2}zE(z)\mathrm{d}z}{\int_{-H/2}^{H/2}E(z)\mathrm{d}z} \tag{2}$$

根据经典梁理论,梁的位移函数为

$$\begin{aligned}u(x,z,t)&=u_0(x,t)-(z-z_0)\frac{\partial w_0(x,t)}{\partial x}\\ w(x,z,t)&=w_0(x,t)\end{aligned} \tag{3}$$

湿热环境下系统的横向应变方程为

$$\varepsilon_x=\varepsilon_{xx}-\varepsilon_x^T-\varepsilon_x^S \tag{4}$$

其中, ε_x^T 和 ε_x^S 分别是梁的热应变和湿应变

$$\varepsilon_x^T=\alpha\Delta T,\qquad \varepsilon_x^S=\beta\Delta S \tag{5}$$

其中 ΔT 和 ΔS 分别代表温度和湿度的变化量.

根据冯卡门几何大变形理论,梁的几何方程为

$$\sigma_x=E(z)\varepsilon_x,\qquad \varepsilon_{xx}=\frac{\partial u}{\partial x}+\frac{1}{2}\left(\frac{\partial w}{\partial x}\right)^2 \tag{6}$$

内力表达式

$$\begin{aligned}N_x&=\int_A\sigma_x\mathrm{d}A\\&=A_x\left[\frac{\partial u_0}{\partial x}+\frac{1}{2}\left(\frac{\partial w_0}{\partial x}\right)^2\right]-N^T-N^S\\ M_x&=\int_A\sigma_x(z-z_0)\mathrm{d}A\\&=-D_x\frac{\partial^2 w}{\partial x^2}-M^T-M^S\end{aligned} \tag{7}$$

其中

$$\begin{aligned}&A_x=\int_A E(z)\mathrm{d}A, D_x=\int_A(z-z_0)^2E(z)\mathrm{d}A\\ &N^T=\Delta T\int_A[E(z)\alpha(z)]\mathrm{d}A\\ &N^S=\Delta S\int_A[E(z)\beta(z)]\mathrm{d}A\end{aligned}$$

$$M^T=\Delta T\int_A(z-z_0)[E(z)\alpha(z)]\mathrm{d}A$$

$$M^S=\Delta S\int_A(z-z_0)[E(z)\beta(z)]\mathrm{d}A$$

假设梁上施加的外力是均匀分布的谐波激励 $q=F_0\cos(\omega t)$,根据广义哈密顿原理,得到系统的动力学方程为

$$\int_{t0}^{t1}(\delta T-\delta U+\delta W+\delta W_{st})\mathrm{d}t=0 \tag{8}$$

其中 T 代表动能,U 表示势能,W 表示外部激振力做的功,W_{st} 为钢丝绳阻尼力做功

$$\begin{aligned}T&=\frac{1}{2}\int_v\rho(z)\left[\left(\frac{\partial u}{\partial x}\right)^2+\left(\frac{\partial w}{\partial x}\right)^2\right]\mathrm{d}V\\U&=\frac{1}{2}\int_v\sigma_x\varepsilon_x\mathrm{d}V\end{aligned} \tag{9}$$

其计算表达式为

$$\begin{aligned}\delta T=&\int_L\left[I_0\left(\frac{\partial u_0}{\partial t}\delta\frac{\partial u_0}{\partial t}+\frac{\partial w_0}{\partial t}\delta\frac{\partial w_0}{\partial t}\right)-\right.\\&I_1\left(\frac{\partial u_0}{\partial t}\delta\frac{\partial^2 w_0}{\partial x\partial t}+\frac{\partial^2 w_0}{\partial x\partial t}\delta\frac{\partial u_0}{\partial t}\right)+\\&\left.I_2\frac{\partial^2 w_0}{\partial x\partial t}\delta\frac{\partial^2 w_0}{\partial x\partial t}\right]\mathrm{d}x\\\delta U=&\int_L\left[N_x\delta\frac{\partial u_0}{\partial x}+\frac{1}{2}N_x\delta\left(\frac{\partial w_0}{\partial x}\right)^2-\right.\\&\left.M_x\delta\frac{\partial^2 w_0}{\partial x^2}\right]\mathrm{d}x\\\delta W=&\int_0^L\left(q-\eta\frac{\partial w_0}{\partial t}\right)\delta w_0\mathrm{d}x\end{aligned}$$

$$\delta W_{st}=\int_0^L(-\chi f_{st})\delta w_0\mathrm{d}x \tag{10}$$

其中 $(I_0,I_1,I_2)=\int_{-H/2}^{H/2}\rho(z)[1,(z-z_0),(z-z_0)^2]\mathrm{d}A$,$\eta$ 是 FGM 梁的阻尼系数,χ 是钢丝绳的阻尼力的修正参数,取 $\chi=0.2$.此外,NiTi-ST 提供的阻尼力可以表示为[21]

$$f_{st}=(1-r)k_3w^3+r(k_ew+z_h) \tag{11}$$

式中 r,k_3,k_e 为实验识别得的参数.z_h 是基于一种修正的 Bouc-Wen 模型的迟滞阻尼力,由下式控制

$$\begin{cases}\dot z_h=\{k_dh(x)-[\gamma+\beta\mathrm{sgn}(z_h\dot w)]\,|z_h|^n\}\dot w\\h(x)=1-\xi\mathrm{e}^{-\frac{w^2}{w_c}}\end{cases} \tag{12}$$

其中,k_d,γ,β,n,ξ,w_c 均为实验识别得的参数;$\dot z_h$ 表示迟滞阻尼力 z_h 对时间求偏导数;$h(x)$ 是用于修正 Bouc-Wen 模型的“收缩效应”函数.然而,钢丝绳的阻尼力以微分方程的形式施加到梁模型中,极大地增加了整个系统的复杂性.因此,基于恢复力曲面法的思想,利用曲线拟合的方法,将钢丝绳的阻尼力表示为关于速度和位移的显式二维多项式,其结果如下[26]

$$\begin{aligned}f_{st}=&k_1w_0+k_3w_0^3+c_1\dot w_0+\\&r_{21}w_0^2\dot w_0+r_{12}w_0\dot w_0^2\end{aligned} \tag{13}$$

基于钢丝绳恢复力和阻尼力的多项式拟合方法,表 1 列出了钢丝绳的曲线拟合参数.

表 1　NiTi-ST 恢复力和阻尼力拟合后的配置参数

Table 1　Configuration parameters of NiTi-ST restoring force and damping force after fitting

Configuration	$k_1\left(\frac{N}{m}\right)$	$k_3\left(\frac{N}{m^3}\right)$	$c_1\left(\frac{N\cdot s}{m}\right)$	$r_{21}\left(\frac{N\cdot s}{m^3}\right)$	$r_{12}\left(\frac{N\cdot s^2}{m^3}\right)$	R-Square
S1a	0	4.097×10^8	122.4	1.699×10^6	-6.515×10^4	0.9983

将公式(10)和公式(12)代入到公式(8)中,同时忽略系统轴向位移的影响,得到

$$\begin{aligned}\delta w_0:&-\frac{\partial}{\partial x}\left(N_x\frac{\partial w_0}{\partial x}\right)-\frac{\partial^2M_x}{\partial x^2}+I_0\frac{\partial^2w_0}{\partial t^2}-\\&I_2\frac{\partial^4w_0}{\partial x^2\partial t^2}+\eta\frac{\partial w_0}{\partial t}-q+\chi f_{st}=0\end{aligned} \tag{14}$$

将内力表达式(7)代入公式(14)中得到 FGM 梁与 NiTi-ST 耦合系统的动力学方程为

$$\begin{aligned}&I_0\frac{\partial^2w_0}{\partial t^2}-I_2\frac{\partial^4w_0}{\partial x^2\partial t^2}+D_x\frac{\partial^4w_0}{\partial x^4}-\\&\frac{3}{2}A_x\frac{\partial^2w_0}{\partial x^2}\left(\frac{\partial w_0}{\partial x}\right)^2+N^T\frac{\partial^2w_0}{\partial x^2}+N^S\frac{\partial^2w_0}{\partial x^2}+\\&\eta\frac{\partial w_0}{\partial t}-F_0\cos(\omega t)+\chi f_{st}=0\end{aligned} \tag{15}$$

边界条件为

$$\begin{aligned}&w_0(0,t)=0,w_0'(0,t)=0\\&w_0(L,t)=0,w_0'(L,t)=0\end{aligned} \tag{16}$$

将方程无量纲化,并引入以下无量纲量

$$\bar x=\frac{x}{L},\bar w_0=\frac{w_0}{L},\bar t=\frac{t}{L^2}\sqrt{\frac{D_x}{I_0}},\bar\omega=\omega L^2\sqrt{\frac{I_0}{D_x}}$$

$$\bar{I}_2=\frac{I_2}{I_0L^2},\bar{A}_x=\frac{A_xL^2}{D_x},\bar{N}^T=\frac{N^TL^2}{D_x}$$

$$\bar{N}^S=\frac{N^SL^2}{D_x},\bar{\eta}=\frac{\eta}{L}\sqrt{\frac{1}{D_xI_0}},\bar{F}_0=\frac{F_0L^3}{D_x}$$

$$\bar{k}_1=k_1\frac{L^4}{D_x},\bar{k}_3=k_3\frac{L^6}{D_x},\bar{c}_1=cL^2\sqrt{\frac{1}{D_xI_0}}$$

$$\bar{r}_{21}=r_{21}L^3\sqrt{\frac{1}{D_xI_0}},\bar{r}_{12}=r_{12}\frac{L}{I_0} \tag{17}$$

对方程进行无量纲处理,得到的无量纲化动力学方程为

$$\frac{\partial^2\bar{w}_0}{\partial\bar{t}^2}-\bar{I}_2\frac{\partial^4\bar{w}_0}{\partial\bar{x}^2\partial\bar{t}^2}+\frac{\partial^4\bar{w}_0}{\partial\bar{x}^4}-\frac{3}{2}\bar{A}_x\frac{\partial^2\bar{w}_0}{\partial\bar{x}^2}\left(\frac{\partial\bar{w}_0}{\partial\bar{x}}\right)^2+$$
$$\bar{N}^T\frac{\partial^2\bar{w}_0}{\partial\bar{x}^2}+\bar{N}^S\frac{\partial^2\bar{w}_0}{\partial\bar{x}^2}+\bar{\eta}\frac{\partial\bar{w}_0}{\partial\bar{t}}-$$
$$\bar{F}_0\cos(\bar{\omega}\bar{t})+\chi\bar{f}_{st}=0$$
$$\bar{f}_{st}=\bar{k}_1\bar{w}_0+\bar{k}_3\bar{w}_0^3+\bar{c}_1\dot{\bar{w}}_0+\bar{r}_{21}\bar{w}_0^2\dot{\bar{w}}_0+\bar{r}_{12}\bar{w}_0\dot{\bar{w}}_0^2 \tag{18}$$

无量纲化后的边界条件为

$$\bar{w}_0(0,\bar{t})=0,\bar{w}_0'(0,\bar{t})=0$$
$$\bar{w}_0(1,\bar{t})=0,\bar{w}_0'(1,\bar{t})=0 \tag{19}$$

2 梁自由振动分析

忽略方程的非线性项、外激励项和钢丝绳恢复力项,得到相对应的梁的自由振动控制方程

$$\frac{\partial^4\bar{w}_0}{\partial\bar{x}^4}+\frac{\partial^2\bar{w}_0}{\partial\bar{t}^2}=0 \tag{20}$$

假设方程的解为

$$\bar{w}_0(x,t)=\phi(\bar{x})q(\bar{t})=(C_1\cos\beta x+C_2\sin\beta x+$$
$$C_3\mathrm{ch}\beta x+C_4\mathrm{sh}\beta x)q(\bar{t}) \tag{21}$$

其中,$q(\bar{t})$ 为广义坐标,$\phi(\bar{x})$ 为模态函数,特征值和固有频率之间的关系为

$$\beta^4=\omega_n^2 \tag{22}$$

将解代入到无量纲后的边界条件中,并将方程整理成下式为

$$\begin{bmatrix}1&0&1&0\\ \cos\beta&\sin\beta&\cosh\beta&\sinh\beta\\ -\beta\sin\beta&\beta\cos\beta&\beta\sinh\beta&\beta\cosh\beta\\ 0&\beta&0&\beta\end{bmatrix}\begin{bmatrix}C_1\\C_2\\C_3\\C_4\end{bmatrix}=0 \tag{23}$$

令上式的系数矩阵行列式值为零,可以求得特征值 β 的值,进而通过式(22)得到系统的各阶固有频率.系数 $C_j(j=1,2,3,4)$ 为常数,可由下式得到.

$$C_1=C_1$$
$$C_2=-\frac{C_1(\cos\beta-\cosh\beta)}{\sin\beta-\sinh\beta}$$
$$C_3=-C_1$$
$$C_4=\frac{C_1(\cos\beta-\cosh\beta)}{\sin\beta-\sinh\beta} \tag{24}$$

进而得到梁自由振动的固有频率和模态函数.图 2 显示了梁自由振动的模态函数.FGM 梁材料选为铝和氧化铝,其材料参数如表 2 所示.

表 2 材料参数

Table 2 Material parameters

Item	Notation	Value
Length	L	1m
Width	B	0.04m
Height	H	0.01m
Ceramic's young modulus	E_1	380GPa
Metal's young modulus	E_2	70GPa
Ceramic's density	ρ_1	3800kg/m^3
Metal's density	ρ_2	2700kg/m^3
Ceramic's thermal expansion coefficient	α_1	7.4×10^{-6}K^{-1}
Metal's thermal expansion coefficient	α_2	2.3×10^{-5}K^{-1}
Ceramic's humidity expansion coefficient	β_1	0
Metal's humidity expansion coefficient	β_2	0.0033
Gradient index	n	1
Damping coefficient	η	5Ns/m

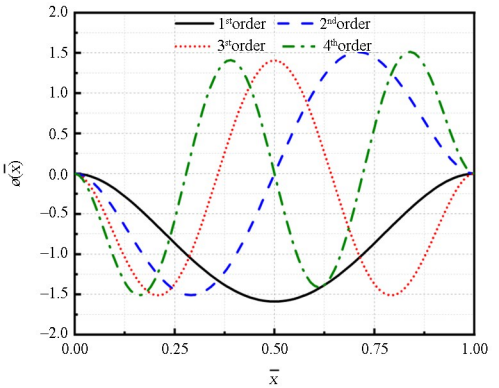

图 2 模态图

Fig.2 Diagram of modal function

3 梁受迫振动分析

3.1 伽辽金法(GTM)

由于系统的控制方程(18)是一组偏微分方程,用 GTM 近似求解,设解的形式为

$$\bar{w}_0(\bar{x},\bar{t})=\sum_{i=1}^{N}\phi_i(\bar{x})q_i(\bar{t}) \tag{25}$$

将式(25)代入式(18)中,并乘以权函数 $\varphi_m(\bar{x})$,权函数被视为是模态函数.然后在[0,1]上积分可得到

$$\int_0^1\sum_{i=1}^{N}\phi_i(\bar{x})\ddot{q}_i(\bar{t})\varphi_m(\bar{x})\mathrm{d}\bar{x}-\bar{I}_2\int_0^1\sum_{i=1}^{N}\phi_i''(\bar{x})\ddot{q}_i(\bar{t})\varphi_m(\bar{x})\mathrm{d}\bar{x}+\int_0^1\sum_{i=1}^{N}\phi_i^{(4)}(\bar{x})q_i(\bar{t})\varphi_m(\bar{x})\mathrm{d}\bar{x}-$$
$$\frac{3}{2}\bar{A}_x\int_0^1\sum_{i=1}^{N}\phi_i''(\bar{x})q_i(\bar{t})[\sum_{i=1}^{N}\phi_i'(\bar{x})q_i(\bar{t})]^2\varphi_m(\bar{x})\mathrm{d}\bar{x}+\bar{N}^T\int_0^1\sum_{i=1}^{N}\phi_i''(\bar{x})q_i(\bar{t})\varphi_m(\bar{x})\mathrm{d}\bar{x}+$$
$$\bar{N}^S\int_0^1\sum_{i=1}^{N}\phi_i''(\bar{x})q_i(\bar{t})\varphi_m(\bar{x})\mathrm{d}\bar{x}+\bar{\eta}\int_0^1\sum_{i=1}^{N}\phi_i(\bar{x})\dot{q}_i(\bar{t})\varphi_m(\bar{x})\mathrm{d}\bar{x}-\bar{F}_0\cos(\bar{\omega}\bar{t})\int_0^1\sum_{i=1}^{N}\varphi_m(\bar{x})\mathrm{d}\bar{x}+$$
$$\chi\{\bar{k}_1\int_0^1\sum_{i=1}^{N}\phi_i(\bar{x})q_i(\bar{t})\varphi_m(\bar{x})\mathrm{d}\bar{x}+\bar{k}_3\int_0^1[\sum_{i=1}^{N}\phi_i(\bar{x})q_i(\bar{t})]^3\varphi_m(\bar{x})\mathrm{d}\bar{x}+$$
$$\bar{c}_1\int_0^1\sum_{i=1}^{N}\phi_i(\bar{x})\dot{q}_i(\bar{t})\varphi_m(\bar{x})\mathrm{d}\bar{x}+\bar{r}_{21}\int_0^1[\sum_{i=1}^{N}\phi_i(\bar{x})q_i(\bar{t})]^2\sum_{i=1}^{N}[\phi_i(\bar{x})\dot{q}_i(\bar{t})]\varphi_m(\bar{x})\mathrm{d}\bar{x}+$$
$$\bar{r}_{12}\int_0^1\sum_{i=1}^{N}[\phi_i(\bar{x})q_i(\bar{t})][\sum_{i=1}^{N}\phi_i(\bar{x})\dot{q}_i(\bar{t})]^2\varphi_m(\bar{x})\mathrm{d}\bar{x})=0 \tag{26}$$

上式可以写为

$$C_{1,i}\ddot{q}_i(\bar{t})+C_{2,i}\dot{q}_i(\bar{t})+C_{3,i}q_i(\bar{t})-F_0\cos(\bar{\omega}\bar{t})C_{4,i}-\frac{3}{2}\bar{A}_x\int_0^1[\sum_{i=1}^{N}\phi_i''(\bar{x})q_i(\bar{t})][\sum_{i=1}^{N}\phi_i'(\bar{x})q_i(\bar{t})]^2\varphi_m(\bar{x})\mathrm{d}\bar{x}+$$
$$\int_0^1\chi f[\sum_{i=1}^{N}\varphi_i(\bar{x})q_i(\bar{t}),\sum_{i=1}^{N}\varphi_i(\bar{x})\dot{q}_i(\bar{t})]\varphi_m(\bar{x})\mathrm{d}\bar{x}=0$$
$$C_{1,i}=\int_0^1\sum_{i=1}^{N}\phi_i(\bar{x})\varphi_m(\bar{x})\mathrm{d}\bar{x}-\bar{I}_2\int_0^1\sum_{i=1}^{N}\phi_i''(\bar{x})\varphi_m(\bar{x})\mathrm{d}\bar{x}$$
$$C_{2,i}=\bar{\eta}\int_0^1\sum_{i=1}^{N}\phi_i(\bar{x})\varphi_m(\bar{x})\mathrm{d}\bar{x}$$
$$C_{3,i}=\int_0^1\sum_{i=1}^{N}\phi_i^{(4)}(\bar{x})\varphi_m(\bar{x})\mathrm{d}\bar{x}+\bar{N}^T\int_0^1\sum_{i=1}^{N}\phi_i''(\bar{x})\varphi_m(\bar{x})\mathrm{d}\bar{x}+\bar{N}^S\int_0^1\sum_{i=1}^{N}\phi_i''(\bar{x})\varphi_m(\bar{x})\mathrm{d}\bar{x}$$
$$C_{4,i}=\int_0^1\varphi_m(\bar{x})\mathrm{d}\bar{x} \tag{27}$$

在后续的求解过程中均采用四阶伽辽金截断,即取 $N=4$

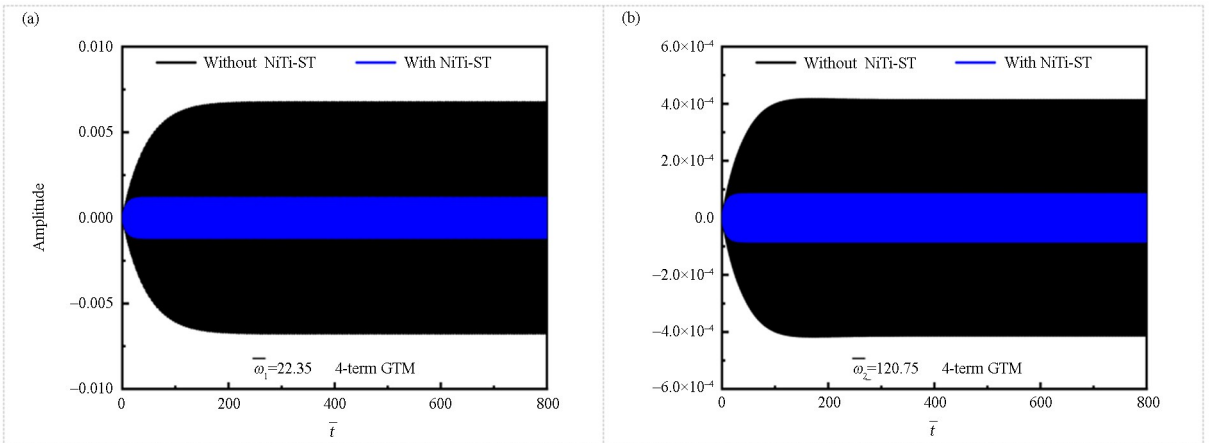

图 3　前两阶共振频率下的时域图 (a)$\bar{\omega}=22.35$ (b)$\omega=120.75$

Fig.3　Time domain diagram at first two order resonance frequencies (a)$\bar{\omega}=22.35$ (b)$\omega=120.75$

图 3 显示了使用 RKM 计算 FGM 梁耦合模型的前两阶共振频率下的时域响应.可以看出,时域解是稳定的,NiTi-ST 对梁的振动抑制有着显著的效果.

3.2　谐波平衡法(HBM)

上一小节通过数值仿真过程研究了 NiTi-ST 对 FGM 梁模型的振动抑制效果.这一节我们采用

谐波平衡法进行近似解析求解,从而得到整个系统的幅频响应曲线.假设系统的解为

$$q_i(\bar{t}) = A_{1,i}\cos(\bar{\omega}\bar{t}) + B_{1,i}\sin(\bar{\omega}\bar{t}) + A_{3,i}\cos(3\bar{\omega}\bar{t}) + B_{3,i}\sin(3\bar{\omega}\bar{t}) \tag{28}$$

通过将式(28)代入式(27),然后使用基于牛顿迭代方法的伪弧长法求解代数方程组.

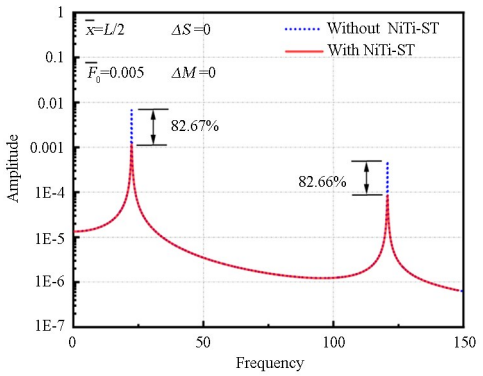

图 4 有无 NiTi-ST 时 FGM 梁的幅频响应曲线对比图

Fig.4 Comparison of amplitude-frequency response curves of FGM beam with and without NiTi-ST

图 4 中采用谐波平衡法对有无 NiTi-ST 的梁模型进行近似解析求解.对图 4 纵轴的振幅作了对数处理,即每一格相差一个数量级.图 4 表明,NiTi-ST 阻尼装置在前两阶共振频率下对耦合梁系统具有良好的减振效果,减振率可达 80%以上.由于第二阶共振峰振幅值与第一阶相比差距很大,所以在后续的研究中主要讨论第一阶共振峰.

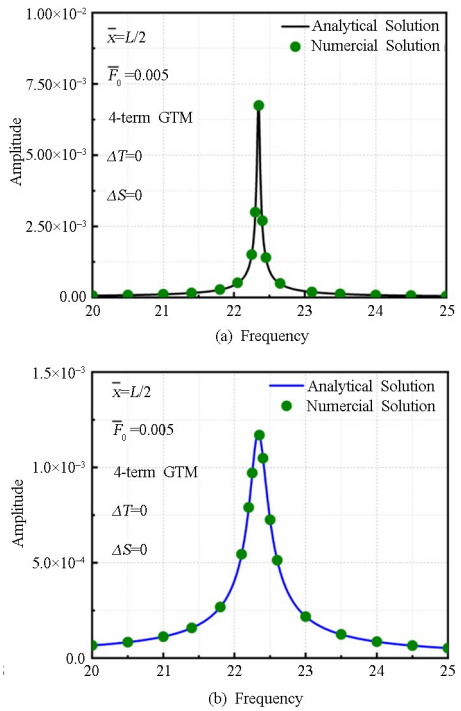

图 5 数值解析对比图.(a)无 NiTi-ST (b)有 NiTi-ST

Fig.5 Comparison of numerical and analytical solutions. (a) Without NiTi-ST (b) With NiTi-ST

图 5 展示了系统在有无 NiTi-ST 装置两种情况下,数值解与近似解析解的对比.图中的实线部分代表 HBM 求得的近似解析解,实心圆点表示是由 RKM 计算求得的数值解.如图所示,两种方法的结果吻合度很高,由此可以验证 HBM 的分析方法的正确性.因此,我们后续使用近似解析解来讨论湿热环境下 NiTi-ST 对 FGM 梁模型的影响.

4 湿热环境下减振效果分析

在温度和湿度变化的过程中,主要影响的是系统的刚度值.由于镍钛合金钢丝绳的刚度与功能梯度梁的刚度相差较大,故不考虑温度和湿度对镍钛合金钢丝绳刚度的影响.

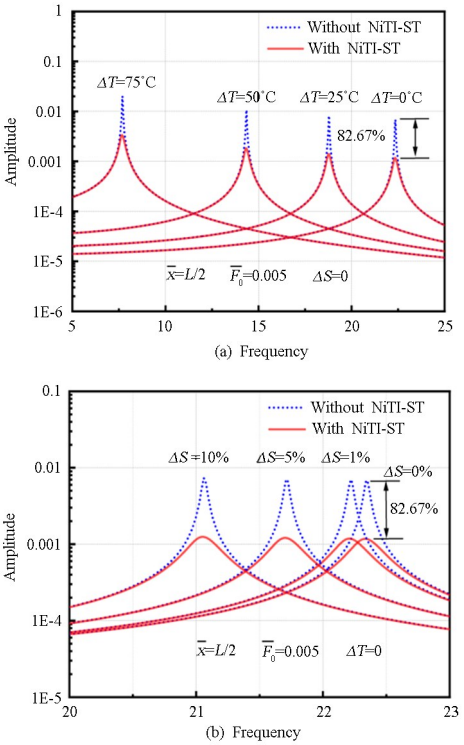

图 6 温湿度对系统振动控制的影响.(a)变温度(b)变湿度

Fig.6 Influence of temperature and humidity on system vibration control.(a) Temperature change (b) Humidity change

图 6(a)显示了改变温度环境,位于梁中点的系统的幅频响应曲线.由图所示,系统的第一阶共振频率随温度变化明显.温度的升高会影响梁本身的结构刚度,从而使模型的固有频率减小,共振峰的峰值随之增大.即使温度升高,系统的共振峰的峰值随之增大,但 NiTi-ST 的减振效果几乎不受温度的影响,基本稳定在 80%上下.因此在一定的温度范围内,NiTi-ST 对系统有着良好的减振效果.

图 6(b)显示了在不同湿度条件下系统的幅频响应曲线.由图所示,湿度对系统共振频率影响很

小,当湿度改变 5%以上,系统固有频率才会有明显的变化,且系统共振峰峰值基本不变.与改变温度相类似,湿度也不会影响 NiTi-ST 的减振效果.所以 NiTi-ST 对不同的湿度环境下也有很出色的减振效果.

5　结论

本文研究湿热环境下 NiTi-ST 和 FGM 梁耦合系统的减振效果.基于广义哈密顿理论,推导了 FGM 梁耦合 NiTi-ST 阻尼器的控制方程.采用 GTM 对偏微分方程进行离散化,得到系统的常微分方程组.采用 RKM 和 HBM 方法分别从数值和分析两个方面计算系统的振动响应.改变外部环境的温度、湿度数值,讨论温度、湿度对 NiTi-ST 减振效果的影响.

本研究的具体结论如下:

(1).NiTi-ST 可以有效抑制谐波激励下耦合梁模型在固有频率附近的振动响应.因此,NiTi-ST 是一种很有前途的阻尼装置.

(2).温度数值的增大,会随之影响梁结构的刚度,固有频率降低,共振峰处的振幅值增大,但 NiTi-ST 的减振效果几乎不受温度的影响.

(3).湿度数值的增大,固有频率变化很小,共振峰处的振幅值变化不大,NiTi-ST 的减振效果几乎不受湿度的影响.

参考文献

[1] 杜长城,李映辉. 功能梯度薄壁圆柱壳的自由振动[J]. 动力学与控制学报, 2010, 8(3): 219－223.
DU C C, LI Y H. Free vibration of functionally graded cylindrical thin shells [J]. Journal of Dynamics and Control, 2010, 8(3): 219－223. (in Chinese)

[2] SINGH B N, RANJAN V, HOTA R N. Vibro-acoustic response of mode localized thin functionally graded plates using physical neutral surface [J]. Composite Structures, 2022, 287: 115301.

[3] SOFIYEV A H. The buckling and vibration analysis of coating-FGM-substrate conical shells under hydrostatic pressure with mixed boundary conditions [J]. Composite Structures, 2019, 209: 686－693.

[4] GAO T, CAO S Q, HOU L L, et al. An experimental study on the nonlinear vibration phenomenon of a rotor system subjected to barrel roll flight and coupled rub-impact faults [J]. Measurements, 2020, 153: 107406.

[5] 李炀,谭霞,丁虎,等. 两端带有弹簧支撑的轴向运动梁振动分析[J]. 动力学与控制学报, 2019, 17(4): 335－340.
LI Y, TAN X, DING H, et al. Nonlinear transverse vibration of an axially moving beam with vertical spring boundary [J]. Journal of Dynamics and Control, 2019, 17(4): 335－340. (in Chinese)

[6] 刘涛,周洋忻,胡伟鹏. 轴向运动功能梯度梁横向振动问题的保结构分析[J]. 动力学与控制学报, 2022, 20(6): 90－95.
Liu T, Zhou Y X, Hu W P. Structure-preserving analysis on transverse vibration of functionally grader beam with an axial velocity [J]. Journal of Dynamics and Control, 2022, 20(6): 90－95. (in Chinese)

[7] 谭霞,丁虎,陈立群. 超临界轴向运动 Timoshenko 梁横向受迫振动[J]. 振动与冲击, 2017, 36(22): 1－5.
TAN X, DING H, CHEN L Q. Transverse forced vibration of an axially moving Timoshenko beam at a supercritical speed [J]. Journal of Vibration and Shock, 2017, 36(22): 1－5.(in Chinese)

[8] TIAN W, ZHAO T, GU Y S, et al. Nonlinear flutter suppression and performance evaluation of periodically embedded nonlinear vibration absorbers in a supersonic FGM plate [J]. Aerospace Science and Technology, 2022, 121: 107198.

[9] CHAARI R, HADDAR M, DJEMAL F, et al. Passive vibration absorber effect on the machining surface quality of a flexible workpiece [J]. Comptes Rendus Mecanique, 2019, 347(12): 903－911.

[10] YANG K, TONG W H, LIN L Q, et al. Active vibration isolation performance of the bistable nonlinear electromagnetic actuator with the elastic boundary [J]. Journal of Sound Vibration, 2022, 520: 116588.

[11] JIANG G Q, WANG Y, LI F M, et al. An integrated nonlinear passive vibration control system and its vibration reduction properties [J]. Journal of Sound Vibration, 2021, 509: 116231.

[12] WANG Y, KLETSCHKOWSKI T. Semi-active vibration control based on a smart exciter with an optimized electrical shunt circuit [J]. Applied Sciences, 2021, 11(20): 9404.

[13] 唐锋,王勇,丁虎,等. 天棚半主动惯容隔振器动态

特性研究 [J]. 振动与冲击，2021，40(15)：65－72.
TANG F，WANG Y，DING H，et al. Dynamic characteristics of skyhook semi-active inerter-based vibration isolator [J]. Journal of Vibration and Shock，2021，40(15)：65－72. (in Chinese)

[14] ZANG J，CAO R Q，ZHANG Y W，et al. A lever-enhanced nonlinear energy sink absorber harvesting vibratory energy via giant magnetostrictive-piezoelectricity [J]. Communications in Nonlinear Science and Numerical Simulation，2021，95：105620.

[15] ZHANG Y W，ZHANG Z，CHEN L Q，et al. Impulse-induced vibration suppression of an axially moving beam with parallel nonlinear energy sinks [J]. Nonlinear Dynamics，2015，82(1)：61－71.

[16] 杨凯，张业伟，丁虎，等. 基于非线性输出频响函数的 NES 动力学参数设计 [J]. 振动与冲击，2016，35(21)：76－80＋86.
YANG K，ZHANG Y W，DING H，et al. Parametric design of nonlinear energy sinks based on nonlinear output frequency-response functions [J]. Journal of Vibration and Shock，2016，35(21)：76－80＋86. (in Chinese)

[17] 尹蒙蒙，丁虎，陈立群. X 型准零刚度隔振器动力学设计及分析 [J]. 动力学与控制学报，2021，19(5)：46－52.
YIN M M，DING H，CHEN L Q. Dynamic design and analysis of X-shaped quasi-zero stiffness isolator [J]. Journal of Dynamics and Control，2021，19(5)：46－52. (in Chinese)

[18] WEN G L，HE J F，LIU J，et al. Design，analysis and semi-active control of a quasi-zero stiffness vibration isolation system with six oblique springs [J]. Nonlinear Dynamics，2021，106(1)：309－321.

[19] OZBULUT O E，HURLEBAUS S，DESROCHES R. Seismic response control using shape memory alloys：a review [J]. Journal of Intelligent Material Systems and Structures，2011，22(14)：1531－1549.

[20] CARBONI B，LACARBONARA W. A new vibration absorber based on the hysteresis of multi-configuration NiTiNOL-steel wire ropes assemblies [C]. MATEC Web of Conferences，2014，16：01004.

[21] CARBONI B，LACARBONARA W，AURICCHIO F. Hysteresis of multiconfiguration assemblies of nitinol and steel strands：experiments and phenomenological identification [J]. Journal of Engineering Mechanics，2015，141(3)：04014135.

[22] CARBONI B，LACARBONARA W. Nonlinear dynamic characterization of a new hysteretic device：experiments and computations [J]. Nonlinear Dynamics，2016，83(1)：23－39.

[23] CARBONI B，LACARBONARA W. Nonlinear vibration absorber with pinched hysteresis：theory and experiments [J]. Journal of Engineering Mechanics，2016，142(5)：04016023.

[24] BREWICK P T，MASRI S F，CARBONI B，et al. Enabling reduced-order data-driven nonlinear identification and modeling through naïve elastic net regularization [J]. International Journal of Non-Linear Mechanics，2017，94：46－58.

[25] CARBONI B，LACARBONARA W，BREWICK P T，et al. Dynamical response identification of a class of nonlinear hysteretic systems [J]. Journal of Intelligent Material Systems and Structures，2018，29(13)：2795－2810.

[26] ZHENG L H，ZHANG Y W，DING H，et al. Nonlinear vibration suppression of composite laminated beam embedded with NiTiNOL-steel wire ropes [J]. Nonlinear Dynamics，2021，103(3)：2391－2407.